A Hybrid Spline Metamodel for Photovoltaic/Wind/Battery Energy Systems

Malek Zaibi[1,2], Toufik Madani Layadi[3], Gérard Champenois[2], Xavier Roboam[4], Bruno Sareni[4] and Jamel Belhadj[1]
[1]Université de Tunis El Manar, LSE-ENIT, BP 37, 1002 Tunis Le Belvédère, Tunisia
Email: malek.zaibi@univ-poitiers.fr – Jamel.Belhadj@esstt.rnu.tn
[2]Université de Poitiers, LIAS-ENSIP, B25, TSA 41105 86073 Poitiers cedex 9, France
Email: gerard.champenois@univ-poitiers.fr
[3]Université Ferhat Abbas Sétif, Sétif 1, LAS, Sétif, Algeria
Email: layaditm@gmail.com
[4]Université de Toulouse, LAPLACE-ENSEEIHT, 2 Rue Camichel 31071 Toulouse Cedex, France
Email: xavier.roboam@laplace.univ-tlse.fr – bruno.sareni@laplace.univ-tlse.fr

***Abstract*—This paper proposes a metamodel design for a Photovoltaic/Wind/Battery Energy System. The modeling of a hybrid PV/wind generator coupled with two kinds of storage i.e. electric (battery) and hydraulic (tanks) devices is investigated. A metamodel is carried out by hybrid spline interpolation to solve the relationships between several design variables i.e. the design parameters of different subsystems and their associate response variables i.e. system indicators performance. The developed model has been successfully validated under real test conditions.**

***Keywords*—Hybrid power systems, Metamodeling, Battery management systems, Hydraulic systems.**

I. Introduction

For complex systems like renewable energy sources, the design assigns highly computation-intensive process for analyses and simulations. Multiple techniques in engineering design and other disciplines have been developed to reduce the computational burden of evaluating numerous designs. Researchers have employed several metamodeling techniques in design and optimization, among which a simpler approximate model named "metamodel" can replace the original system process [1]. For example, the latter makes use of polynominal functions to solve the relationships between several design variables and one or more response variables. Many authors have suggested various types of metamodels among others: classical polynominal function models [2], stochastic models such as the Kriging interpolation model [3],[4],[5] and artificial neural network models [6], [7]. The aim of the present paper is to introduce another metamodel named as hybrid spline model. Due to the complexity of system (approximation model, design variable and problem formulation) the hybrid spline model will be developed. Hence, we use the metamodel to solve the optimization problem. This paper contains three major parts. First, the hybrid Photovoltaic (PV)/Wind Turbines (WT) sources with battery bank powering electrical and hydraulic loads is presented. Second, the metamodel-based global system process is carried out. The metamodel process is based on three steps: Design space sampling of the real-model, parameter extraction of the metamodel and metamodel validation. Finally, the metamodel is used for assessing the hybrid system performance.

978-1-4799-7947-9/15/$31.00

II. System description

The present system includes hybrid Photovoltaic (PV)/Wind turbines (WT) sources with battery bank powering electrical loads and hydraulic network loads. The latter is composed of water pumping and Reverse Osmosis (RO) desalination unit to produce permeate water. Fig.1 presents the global system architecture. The PV/WT/Battery system consists of photovoltaic panels, wind turbines, battery bank and converters (DC/DC and AC/DC). The brackish water pumping and desalination process are composed of two motor-pumps, RO membrane, two water tanks and two (DC/AC) inverters. The different subsystems are coupled to DC Bus. The meteorological profiles: wind speed (V_{wind}), solar irradiation (I_r) and ambient temperature (T_a) of a typical region (North Tunisia) have been recorded for one year.

A. Hybrid Energy Models

1) PV generator model: The PV generator power is determined from a model as defined in [8]-[9]:

$$P_{PV} = \eta_r \cdot \eta_{pc} \cdot [1 - \beta \cdot (T_c - NOCT)] \cdot A_{PV} \cdot I_r \quad (1)$$

where η_r is PV efficiency, η_{pc} the power tracking equipment efficiency, which is equal to 0.9 with a perfect maximum point tracker, β the temperature coefficient, ranging from 0.004 to 0.006 per °C for silicon cells, $NOCT$ normal operating PV cell temperature (°C), A_{PV} the PV panels area (m^2) and T_c the PV cell temperature (°C) which can be expressed by [10]:

$$T_c = 30 + 0.0175 \cdot (I_r - 300) + 1.14 \cdot (T_a - 25) \quad (2)$$

where T_a denotes the ambient temperature (°C).

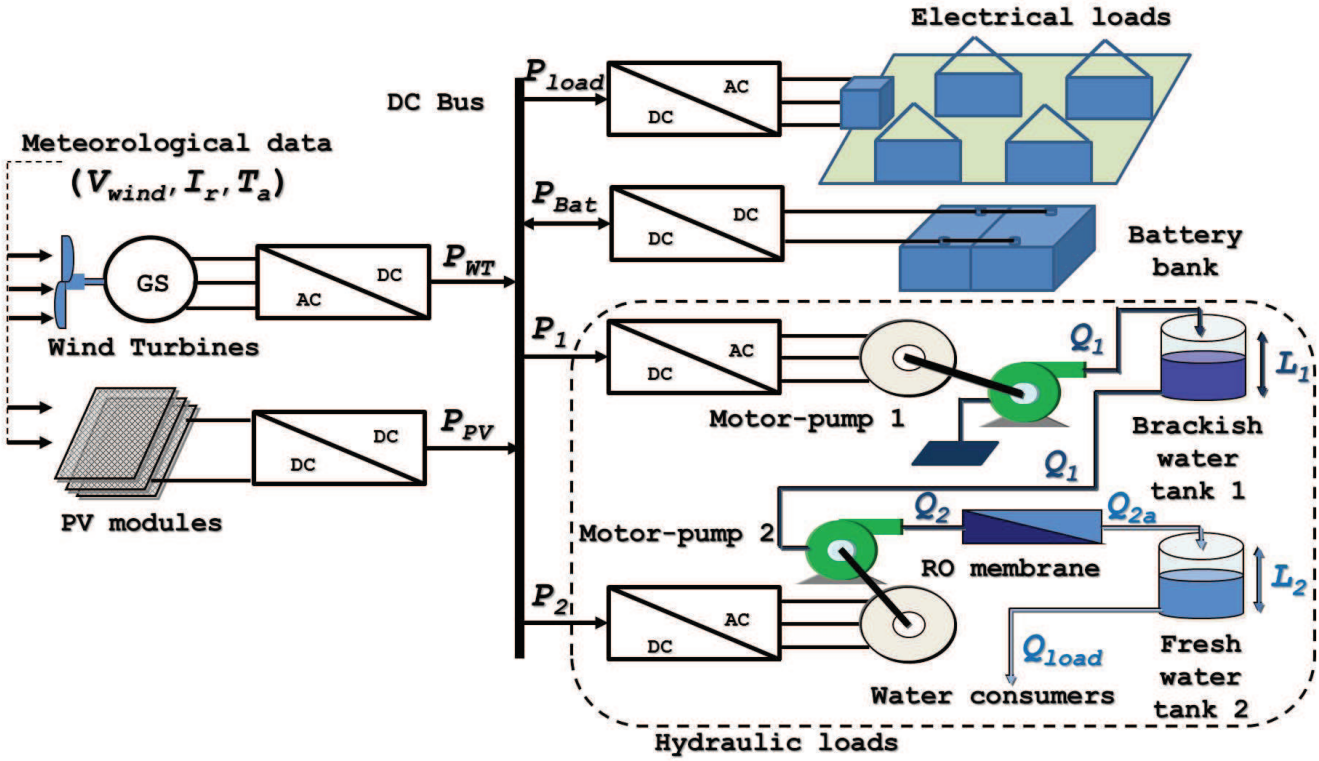

Fig. 1. Global system architecture

2) Wind turbine model: The wind turbine power is expressed as follows [11]:

$$P_{wt} = \frac{1}{2} \cdot C_p \cdot \rho \cdot A_{wt} \cdot V_{wind}^3 \tag{3}$$

where C_p is the wind turbine power coefficient, ρ the air mass density and A_{wt} the wind turbine swept area.

3) Battery storage model: In this study, we propose an ideal model for the battery. During the charging and discharging process, the state of charge (SOC) vs time (t) can be described by [12]:

$$SOC(t) = \left\{ \begin{array}{ll} SOC(t-\Delta t)+ & \eta_{ch} \cdot \frac{P_{Bat}/U_{bus}}{C_n^{Bat}} \cdot \Delta t \\ SOC(t-\Delta t)+ & \frac{1}{\eta_{dis}} \cdot \frac{P_{Bat}/U_{bus}}{C_n^{Bat}} \cdot \Delta t \end{array} \right\} \tag{4}$$

where Δt is the time step (here, three minutes), P_{Bat} represents the battery power, η_{ch} and η_{dis} are respectively the battery efficiencies during charging and discharging phases. U_{bus} denotes the nominal DC bus voltage. C_n^{Bat} represents the nominal capacity of the battery bank in Ampere hour (Ah). At any time step Δt, the SOC must comply with the following constraints:

$$SOC_{min} \leq SOC(t) \leq SOC_{max} \tag{5}$$

where SOC_{min} and SOC_{max} are the minimum and maximum allowable storage capacities, respectively.

4) Electrical load profile: Typical power consumption (P_{load}) data were acquired for a residential home. During 365 days with three minutes acquisition period, this profile describes the weekdays and weekend days consumption (see Fig.2).

B. Hydraulic network models

The hydraulic network is shown in Fig.1. It includes four principal subsystems: the motor-pump 1 which draws water from well, a water storage tank 1, the high pressure motor-pump 2 associated with a reverse osmosis desalination device and a water tank storage 2. this final storage is placed at the output of the desalination process to store fresh water.

1) Model of the motor-pump 1: The GRUNDFOS® motor-pump ("CRN" type) was selected for pumping water from well to the tank water storage 1. The electric power P_1 required for motor-pump 1 at head H and flow rate Q_1 can be calculated as [13]:

$$P_1 = \frac{\rho_w \cdot g \cdot H \cdot Q_1}{\eta_m \cdot \eta_p} \tag{6}$$

where ρ_w is the density of water (kg/m^3), g the gravity constant (m/s^2), η_m the motor efficiency and η_p the pump efficiency.

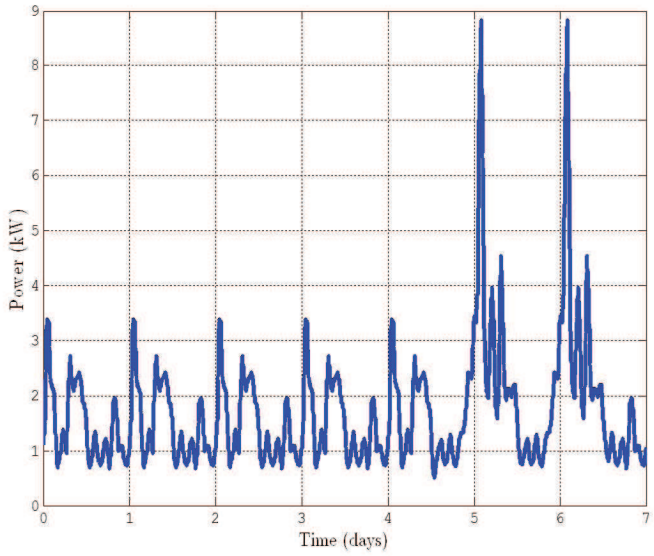

Fig. 2. Weekly power consumption profile

2) Model of the water storage tank 1: Water tank 1 is used to store brackish water. It is characterized by its water level L_1 and its section S_1. The level L_1 can be calculated as follows:

$$L_1(t) = L_1(t - \Delta t) + \frac{(Q_1(t) - Q_2(t))}{S_1} \cdot \Delta t \qquad (7)$$

This tank is fitted with four sensors measuring four different water levels: two minimum sublevels, i.e. high and low (L^1_{minH} and L^1_{minL}) and two maximum sublevels, i.e high and low (L^1_{maxH} and L^1_{maxL}). The high and low levels are separated by a hysteresis band. This hysteresis avoids the switch On/Off of the motor-pump during operation.

3) Model of the motor-pump 2 with reverse osmosis membrane: The GRUNDFOS® motor-pump ("CRN" type) [13] was selected for water pumping from the tank water storage 1 to the tank water storage 2 via a reverse osmosis (RO) desalination system (ROMEMBRA® TORAY RO membrane, "TM" type [14]). In this study, the RO membrane model is characterized by the nominal fresh (permeate) water production in day DM (m^3/d).

Three design configuration between the motor-pumps and RO membrane are used to develop a model (from a fitting approach). Fig.3 presents three RO membrane characteristics $H_2(Q_2)$ and the Fig.4 shows three motor-pump characteristics $P_2(Q_2)$ with their efficiencies.

The expression of the flow rate Q_2 is a function of the electric power P_2 and the nominal fresh water DM:

$$Q_2 = 4.77 \cdot 10^{-6} \cdot P_2^{0.54} \cdot DM^{2.843} + 0.025 \cdot P_2^{0.578} \qquad (8)$$

Moreover, the expression of the minimal and maximal electrical powers, respectively P_2^{min} and P_2^{max} is a function of the nominal fresh water DM:

$$\begin{cases} P_2^{min} = & 53.64 \cdot DM^{0.63} \\ P_2^{max} = & 384 \cdot DM^{0.93} \end{cases} \qquad (9)$$

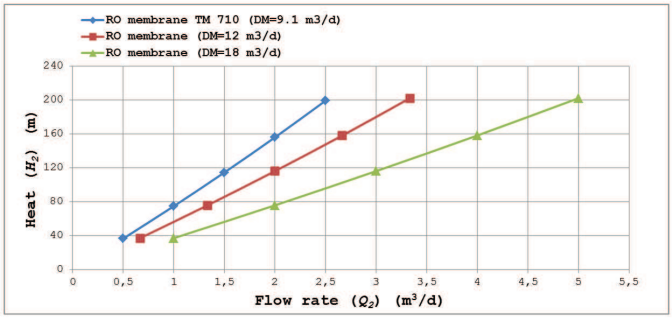

Fig. 3. Different RO membrane characteristics

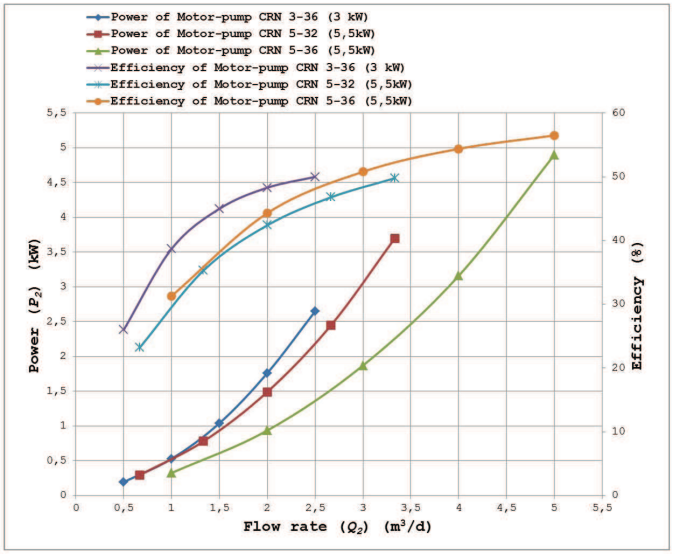

Fig. 4. Different motor-pump characteristics

For the RO process, the flow rate Q_2 is separated between the permeate flow Q_{2a} and the concentrate flow Q_{2b}.

$$\begin{cases} Q_{2a} = & T_c \cdot Q_2 \\ Q_{2b} = & Q_2 - Q_{2a} \end{cases} \qquad (10)$$

where T_c is the conversion rate of the RO membrane (i.e. T_c=20%).

4) Modeling of the fresh water storage tank 2: Water storage tank 2 is the tank of the permeate (fresh) water. It is characterized by the level L_2 and section S_2. The level L_2 can be calculated as follows:

$$L_2(t) = L_2(t - \Delta t) + \frac{(Q_{2a}(t) - Q_{load}(t))}{S_2} \cdot \Delta t \qquad (11)$$

where Q_{load} is the water flow demand required by the consumers. Fig.5 represents the daily water flow demand.

As previously, this tank is fitted with four level sensors: two useful levels, i.e. high and low (L^2_{uH} and L^2_{uL}) and two maximum levels, i.e. high and low (L^2_{maxH} and L^2_{maxL}). The high and low levels are also determined by a hysteresis band.

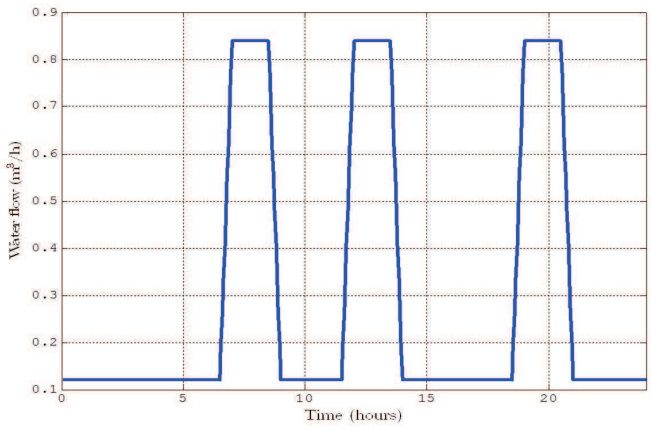

Fig. 5. Daily water flow profile

C. System indicators performance

To assess the performance of this complex system, three indicators are used as follows:

1) The Loss of electric Power Supply Probability ($LPSP_E$),

$$LPSP_E(\%) = \frac{\sum_{\Delta t=1}^{T} \Delta P(\Delta t) \cdot \Delta t}{\sum_{\Delta t=1}^{T} P_{load}(\Delta t) \cdot \Delta t} \tag{12}$$

with

$$\Delta P = \begin{cases} P_{load} - P_{re}, & SOC \leq SOC_{min} \\ 0, & otherwise \end{cases} \tag{13}$$

where P_{re} is the renewable source power and P_{load} is the electrical load power.

2) The Loss of hydraulic Power Supply Probability ($LPSP_H$),

$$LPSP_H(\%) = \frac{\sum_{\Delta t=1}^{T} Q(\Delta t) \cdot \Delta t}{Q_{load} \cdot T} \tag{14}$$

where

$$Q = \begin{cases} Q_{load}, & L_2 = 0 \\ 0, & otherwise \end{cases} \tag{15}$$

3) The exchange energy by the battery ($E_{exchange}$)

$$E_{exchange}(kWh) = \int_0^T |P_{Bat}| \cdot dt \tag{16}$$

To obtain the performance of the three system indicators, a dynamic simulator is developed using MATLAB® environment[12]. The different models of the studied system are integrated in the dynamic simulator. The latter during one year with sample time of three minutes allows us to simulate the system evolution.

III. Metamodel-based process

The proposed metamodel process is summarized in Fig.6. The first step resides in the sampling of the design space with the dynamic simulator. Then the building of the metamodel is performed to deduce the predicted responses. finally the validation step of the metamodel is presented.

A. Design Space Sampling

The relationships between the design variables and the system indicators performance characterized from the dynamic simulator. Given a set of m design sites $S = [s_1 \dots s_m]^T$ with $s_i \in \Re^n$ (n: numbers of design variables) and responses $Y = [y_1 \dots y_m]^T$ with $y_i \in \Re^p$ (p: numbers of responses). For the design site s_i, the design variables is,

$$s_i = \left[A_{pv}, A_{wt}, C_n^{Bat}, SOC_u, L_u^2, S_2, P_1, DM\right]_i \tag{17}$$

The responses y_i versus the system indicators performance are,

$$y_i = \left[LPSP_E, LPSP_H, E_{exchange}\right]_i \tag{18}$$

The space filling design, the sample points around the border and only put few points in the interior of the design space:

$$S = \begin{pmatrix} A_{pv} : x_1 = \{x_1^{min}, \frac{x_1^{min}+x_1^{max}}{2}, x_1^{max}\} \\ A_{wt} : x_2 = \{x_2^{min}, \frac{x_2^{min}+x_2^{max}}{2}, x_2^{max}\} \\ C_n^{Bat} : x_3 = \{x_3^{min}, \frac{x_3^{min}+x_3^{max}}{2}, x_3^{max}\} \\ SOC_u : x_4 = \{x_4^{min}, \frac{x_4^{min}+x_4^{max}}{2}, x_4^{max}\} \\ L_u^2 : x_5 = \{x_5^{min}, \frac{x_5^{min}+x_5^{max}}{2}, x_5^{max}\} \\ S_2 : x_6 = \{x_6^{min}, \frac{x_6^{min}+x_6^{max}}{2}, x_6^{max}\} \\ P_1 : x_7 = \{x_7^{min}, \frac{x_7^{min}+x_7^{max}}{2}, x_7^{max}\} \\ DM : x_8 = \{x_8^{min}, \frac{x_8^{min}+x_8^{max}}{2}, x_8^{max}\} \end{pmatrix} \tag{19}$$

B. Parameter extraction of the Metamodel

The design space data were used for the model fitting to explore the best polynomial function. Those data were employed using MATLAB® Model-Based Calibration Toolbox. In this toolbox, two main global linear models are developed such as polynomial or hybrid splines. After testing these models, the hybrid splines models are used to predict the system indicators performance. The hybrid spline model is a piecewise polynomial function, where different sections of polynomial are fitted smoothly together. The locations of the breaks are called knots. The required number of knots (up to a maximum of 50) and their positions are chosen. In this case all the pieces of curves between the knots are formed from polynomial of the same order (the order up to 3).

C. Metamodel validation

The predicted responses obtained from the hybrid spline model were compared with simulator dynamic responses for testing and validating the metamodel. Different points are used to validate the metamodel. There are two measures of the accurate model, defined as below:

- The Root Mean Square Error ($RMSE$) is:

$$RMSE = \sqrt{\frac{\sum_{i=1}^{N} (y_i - \widehat{y}_i)^2}{N}} \tag{20}$$

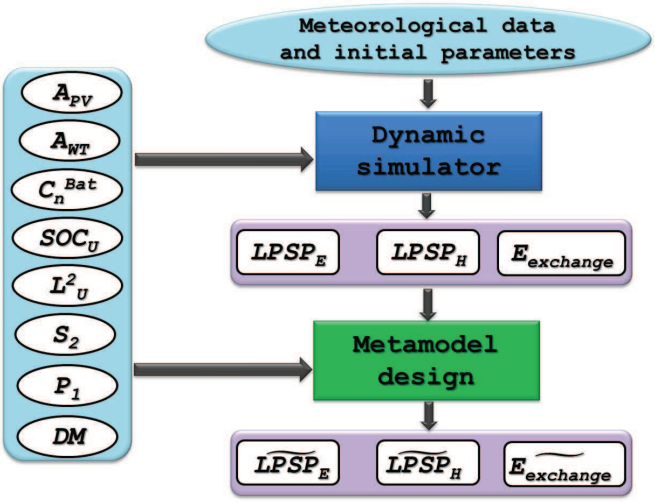

Fig. 6. Metamodel design process

- The R square value, coefficient of determination, (R^2) is:

$$R^2 = 1 - \frac{\sum_{i=1}^{N}(y_i - \widehat{y}_i)^2}{\sum_{i=1}^{N}(y_i - \overline{y})^2} \tag{21}$$

where N is the number of validation points; $\widehat{y}_i$ is the predicted value for the observed value y_i; $\overline{y}$ is the mean of the observed values at the validation points.

IV. Results and Discussion

Following the proposed process, the constraints of the design variables are defined as

$$\begin{cases} 30\ \text{m}^2 \leq A_{pv} \leq 90\ \text{m}^2 \\ 60\ \text{m}^2 \leq A_{wt} \leq 220\ \text{m}^2 \\ 400\ \text{Ah} \leq C_n^{Bat} \leq 600\ \text{Ah} \\ 30\ \% \leq SOC_u \leq 100\ \% \\ 0.3\ \text{m} \leq L_u^2 \leq 1.9\ \text{m} \\ 2\ \text{m}^2 \leq S_2 \leq 20\ \text{m}^2 \\ 600\ \text{W} \leq P_1 \leq 1600\ \text{W} \\ 7\ \text{m}^3/\text{d} \leq DM \leq 30\ \text{m}^3/\text{d} \end{cases} \tag{22}$$

For each design variable, three values (minimal, mean and maximal) are used to obtain the following design space S,

$$S = \begin{pmatrix} A_{pv} = \{30, 60, 90\}\ [\text{m}^2] \\ A_{wt} = \{60, 140, 220\}\ [\text{m}^2] \\ C_n^{Bat} = \{400, 500, 600\}\ [\text{Ah}] \\ SOC_u = \{30, 65, 100\}\ [\%] \\ L_u^2 = \{0.3, 1.1, 1.9\}\ [\text{m}] \\ S_2 = \{2, 11, 20\}\ [\text{m}^2] \\ P_1 = \{600, 1100, 1600\}\ [\text{W}] \\ DM = \{7, 18, 30\}\ [\text{m}^3/\text{d}] \end{pmatrix} \tag{23}$$

Therefore, 6561 (3^8) design configurations are simulated by the dynamic simulator. Then, the system indicators performance (i.e. responses) are deduced for these design sites. The

TABLE I. Results of metamodels measures

	$LPSP_E$	$LPSP_H$	$E_{exchange}$
R^2	0.978	0.949	0.994
$RMSE$	0.336	3.958	52.495

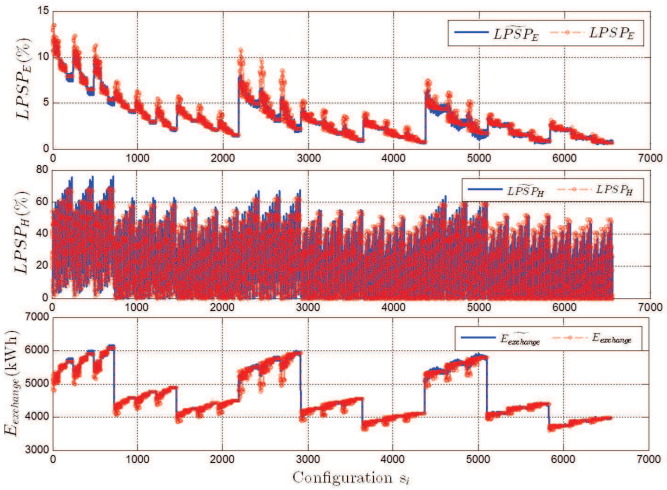

Fig. 7. Predicted responses based on hybrid spline model

TABLE II. CPU Time of dynamic simulator and hybrid spline metamodel

Technique	CPU Time for 6561 design configurations
Dynamic simulator	34769 s
Hybrid spline metamodel	19 s

expressions of the predicted system indicators performance are,

$$\begin{cases} \widetilde{LPSP}_E = & f_1(A_{pv}, A_{wt}, C_n^{Bat}, SOC_u, L_u^2, S_2, P_1, DM, \phi) \\ \widetilde{LPSP}_H = & f_2(A_{pv}, A_{wt}, C_n^{Bat}, SOC_u, L_u^2, S_2, P_1, DM, \phi) \\ \widetilde{E_{exchange}} = & f_3(A_{pv}, A_{wt}, C_n^{Bat}, SOC_u, L_u^2, S_2, P_1, DM, \phi) \\ \phi = & B(A_{wt}, n_{knot}) \end{cases} \tag{24}$$

where f_1, f_2 and f_3 are the second-order polynomial functions; ϕ is the B-spline function: degree 1, n_{knot} is the number of knots ($n_{knot} = 1$) and the knot position is the mean of A_{wt}. This metamodel design along with the predicted responses is shown in Fig.7 and an illustration example for 100 design configurations is presented in Fig. 8.

Table I and Fig.7 show that the hybrid spline metamodels performed quite well leading to a coefficient of determination close to 1 and small values of the $RMSE$ measure. It can be noted that first and second system performance indicators (i.e. $LPSP_E$ and $LPSP_H$) are better interpolated than the third performance criterion (i.e. $E_{exchange}$).

In Table. II, the comparative CPU Time between the dynamic simulator and the hybrid spline model is presented. This results shows the most advantage of the hybrid spline metamodel when using a high number of system simulations such as the optimization process.

V. Conclusion

This work provides an application of the metamodel design for a Photovoltaic/Wind/Battery energy system. The develop-

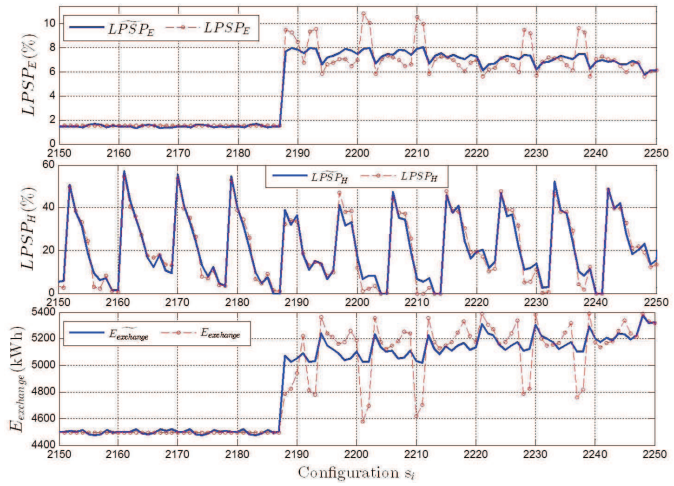

Fig. 8. An illustration of predicted responses (100 design configurations)

ment in metamodelling is categorized according to the complexity of system: approximation model, design variable and problem formulation. Future developments will aim to use the metamodel instead of the dynamic simulator in an optimization process requiring a high number of system simulations. Such approach will benefit of the significant reduction of the CPU time and allow finding optimal configurations of the hybrid system with regard to the performance criteria.

ACKNOWLEDGMENT

The authors would like to thank the CMCU UTIQUE Program for financial support. This work was supported by the Tunisian Ministry of High Education and Research under Grant LSE-ENIT-LR 11ES15.

REFERENCES

[1] G. G. Wang and S. Shan, "Review of metamodeling techniques in support of engineering design optimization," *J. of Mechanical Design*, vol. 129, pp. 370–380, 2006.

[2] F. Chlelaa, A. Husaunndeeb, C. Inardc, and P. Riederera, "A new methodology for the design of low energy buildings," *Energy and Buildings*, vol. 41, pp. 982–990, 2009.

[3] R. Coelho and P. Bouillard, "Multi-objective reliability-based optimization with stochastic metamodels," *Evolutionary Computation*, vol. 19, pp. 525–560, 2014.

[4] H. Wang, E. Li, G. Y. Li, and Z. H. Zhong, "Development of metamodeling based optimization system for high nonlinear engineering problems," *Advances in Engineering Software*, vol. 39, pp. 629–645, 2008.

[5] X. G. Song, L. Wang, S. H. Baek, and Y. C. Park, "Multidisciplinary optimization of a butterfly valve," *ISA Trans.*, vol. 48, pp. 370–377, 2009.

[6] E. Betiku and A. E. Taiwo, "Modeling and optimization of bioethanol production from breadfruit starch hydrolyzate vis-à-vis response surface methodology and artificial neural network," *J. Renew. Energy*, vol. 74, pp. 87–94, 2015.

[7] K. Fang, L. Runze, and A. Sudjianto, *Design and Modeling for Computer Experiments*, T. . F. Group, Ed. Chapman & Hall/CRC, 2006.

[8] J. Hofierka and J. KaÅuk, "Assessment of photovoltaic potential in urban areas using open-source solar radiation tools," *J. Renew. Energy*, vol. 34, no. 10, pp. 2206 – 2214, 2009.

[9] B. Liu, S. Duan, and T. Cai, "Photovoltaic dc building module based bipv system: Concept and design considerations," *IEEE Trans. Power Electronics*, vol. 26 (5), pp. 1418–1429, 2011.

[10] F. Lasnier and T. Ang, *Photovoltaic Engineering Handbook*, 1st ed. Taylor and Francis, 1990.

[11] W. Shepherd and D. Shepherd, *Energy Studies*, 2nd ed. Imperial College Press, 2003.

[12] D. Abbes, A. Martinez, and G. Champenois, "Life cycle cost, embodied energy and loss of power supply probability for the optimal design of hybrid power systems," *J. Math. Comput. Simulat.*, vol. 98, pp. 46–62, 2014.

[13] Grundfos, *The Centrifugal Pump*, 1st ed. Department of Structural and Fluid Mechanics, 2013.

[14] Toray, *Operation, Maintenance and Handling Manual for membrane elements*. Toray Reverse Osmosis Elements, 2012.